

On jet structure in heavy ion collisions

I.P. Lokhtin, A.A. Alkin, A.M. Snigirev

Skobeltsyn Institute of Nuclear Physics, Lomonosov Moscow State University, Moscow, Russia

Abstract. The LHC data on jet fragmentation function and jet shapes in PbPb collisions at center-of-mass energy 2.76 TeV per nucleon pair are analyzed and interpreted in the frameworks of PYQUEN jet quenching model. A specific modification of longitudinal and radial jet profiles in most central PbPb collisions as compared with pp data is close to that obtained with PYQUEN simulations taking into account wide-angle radiative and collisional partonic energy loss. The contribution of radiative and collisional loss to the medium-modified intra-jet structure is estimated.

1 Introduction

Studying the modification of jets as they are formed from energetic partons propagating through the hot and dense medium created in ultrarelativistic heavy ion collisions is a particularly useful tool for probing the produced matter's properties. The energy loss of jet partons in deconfined medium, quark-gluon plasma, is predicted much stronger than in cold nuclear matter, and leads to so called “jet quenching” effect (see, e.g., reviews [1, 2, 3, 4, 5, 6, 7] and references therein). Indirectly jet quenching was observed for the first time at RHIC experiments via measurements of inclusive high- p_T hadron production in gold-gold collisions at center-of-mass energy $\sqrt{s_{NN}} = 200$ GeV. It was manifested as the suppression of overall high- p_T hadron rates and back-to-back dihadron azimuthal correlations (including the specific azimuthal angle dependence of the effect with respect to the event plane). The summary of experimental results at RHIC can be found in [8, 9, 10, 11].

The lead-lead collision energy at LHC, $\sqrt{s_{NN}} = 2.76$ TeV, is a factor of ~ 14 larger than that in RHIC, thereby allows one to probe new frontiers of super-hot quark-gluon matter. The analysis of high statistics samples of fully reconstructed jets becomes possible. The results of jet analyses of 2010 and 2011 PbPb data obtained by three LHC experiments, ALICE, ATLAS and CMS, is summarized e.g. in review [12]. The first direct evidence of jet quenching has been observed as the large, centrality-dependent, imbalance in dijet transverse energy [13, 14]. It has been found using missing p_T techniques that the jet energy loss spreads over low transverse momenta and large angles [14]. Then jet momentum dependence of the dijet imbalance has been studied in detail [15]. Significant transverse energy imbalance has been observed for photon+jet production in PbPb events [16]. Another direct manifestation of jet quenching is the inclusive jet suppression in central PbPb collisions compared to peripheral events [17, 18] and to proton-proton interactions [19]. The azimuthal angle dependence of such suppression has also been mea-

sured [20]. The similar level of suppression as for inclusive jets is seen for jets from b-quark fragmentation [21]. In contrast to PbPb collisions, proton-lead data from LHC do not show jet quenching manifestation [22].

A number of theoretical calculations and Monte-Carlo simulations were attempted to reproduce some of basic features of jet quenching pattern at LHC (dijet and photon+jet imbalance, nuclear modification factors for jets and high- p_T hadrons), and to extract by such a way the information about medium properties and partonic energy loss mechanisms [23, 24, 25, 26, 27, 28, 29, 30, 31, 32, 33, 34, 35, 36, 37, 38, 39, 40, 41, 42]. The observable that allows more precise comparison between the data and theoretical models of jet quenching to be done, is the internal jet structure. The recently published experimental data on medium-modified jet structure include the measurement of jet shapes (radial profile) [43] and jet fragmentation function (longitudinal profile) [44, 45]. It was suggested in [46] that it could be also of interest to study moments of jet fragmentation function.

In present paper, the LHC data on jet fragmentation function and jet shapes in PbPb collisions are analyzed and interpreted in the frameworks of PYQUEN partonic energy loss model [47]. In the previous papers [27, 28] this model were applied to analyze the dijet energy asymmetry and nuclear modification factor of inclusive hadrons.

2 PYQUEN model

PYQUEN (PYthia QUENched) is one of the first Monte-Carlo models of jet quenching [47]. PYQUEN was constructed as a modification of jet events obtained with the generator of hadron-hadron interactions PYTHIA_6.4 [48]. The details of the used physics model and simulation procedure can be found in the original paper [47]. Main features of the model are listed below as follows.

The approach describing the multiple scattering of hard partons relies on accumulated energy loss via gluon radiation, which is associated with each parton scattering in a

hot matter. It also includes the interference effect in gluon emission with a finite formation time using the modified radiation spectrum dE/dl as a function of the decreasing temperature T . The basic kinetic integral equation for the partonic energy loss ΔE as a function of initial energy E and path length L has the form

$$\Delta E(L, E) = \int_0^L dl \frac{dP(l)}{dl} \lambda(l) \frac{dE(l, E)}{dl}, \quad (1)$$

$$\frac{dP(l)}{dl} = \frac{1}{\lambda(l)} \exp(-l/\lambda(l)),$$

where l is the current transverse coordinate of a parton, dP/dl is the scattering probability density, dE/dl is the energy loss per unit length, $\lambda = 1/(\sigma\rho)$ is the in-medium mean free path, $\rho \propto T^3$ is the medium density at the temperature T , σ is the integral cross section for the parton interaction in the medium.

The model takes into account radiative and collisional energy loss of hard partons in longitudinally expanding quark-gluon fluid, as well as the realistic nuclear geometry. The radiative energy loss is treated in the frameworks of BDMPS model [49,50,51]:

$$\frac{dE^{rad}}{dl} = \frac{2\alpha_s(\mu_D^2)C_R}{\pi L} \int_{\mu_D^2 \lambda_g}^E d\omega \left[1 - y + \frac{y^2}{2} \right] \ln |\cos(\omega_1 \tau_1)| \quad (2)$$

$$\omega_1 = \sqrt{i \left(1 - y + \frac{C_R}{3} y^2 \right) \bar{\kappa} \ln \frac{16}{\bar{\kappa}}}, \quad \bar{\kappa} = \frac{\mu_D^2 \lambda_g}{\omega(1-y)},$$

where $\tau_1 = L/(2\lambda_g)$, $y = \omega/E$ is the fraction of the hard parton energy carried away by the radiated gluon, α_s is the QCD running coupling constant for N_f active quark flavors, $C_R = 4/3$ is the quark color factor, and μ_D is the Debye screening mass. A similar expression for the gluon jet can be obtained by setting $C_R = 3$ and properly changing the factor in the square brackets in (2) [50]. The simple generalization to a radiative energy loss of massive quark case uses the “dead-cone” approximation [52].

The collisional energy loss due to elastic scatterings is calculated in the high-momentum transfer limit [53,54,55]:

$$\frac{dE^{col}}{dl} = \frac{1}{4T\lambda\sigma} \int_{\mu_D^2}^{t_{\max}} dt \frac{d\sigma}{dt} t, \quad (3)$$

where the dominant contribution to the differential scattering cross section is

$$\frac{d\sigma}{dt} \cong C \frac{2\pi\alpha_s^2(t)}{t^2} \frac{E^2}{E^2 - m_p^2} \quad (4)$$

for the scattering of a hard parton with energy E and mass m_p off the “thermal” parton with energy (or effective mass) $m_0 \sim 3T \ll E$. Here $C = 9/4, 1, 4/9$ for gg, gq

and qq scatterings respectively. The integrated cross section σ is regularized by the Debye screening mass squared $\mu_D^2(T) \simeq 4\pi\alpha_s T^2(1 + N_f/6)$. The maximum momentum transfer is $t_{\max} = [s - (m_p + m_0)^2][s - (m_p - m_0)^2]/s$ where $s = 2m_0E + m_0^2 + m_p^2$.

The medium where partonic rescattering occurs is considered as a boost-invariant longitudinally expanding perfect quark-gluon fluid, and the partons as being produced on a hyper-surface of equal proper times τ [56]. Then the proper time dependence of a temperature T , energy density ε and number density ρ gets the form:

$$\varepsilon(\tau) = \varepsilon_0 \left(\frac{\tau_0}{\tau} \right)^{4/3}, \quad T(\tau) = T_0 \left(\frac{\tau_0}{\tau} \right)^{1/3}, \quad \rho(\tau) = \rho_0 \frac{\tau_0}{\tau}. \quad (5)$$

In principle, other scenarios of space-time evolution of quark-gluon matter can be considered within PYQUEN model [47]. For example, the presence of fluid viscosity slows down the cooling rate, i.e., in fact the effective temperature gets higher as compared with the perfect fluid case. At the same time, the influence of the transverse expansion of the medium on parton rescattering intensity is practically inessential for high initial temperatures T_0^{\max} .

The strength of partonic energy loss in PYQUEN is determined mainly by the initial maximal temperature T_0^{\max} of hot fireball in central PbPb collisions, which is achieved in the center of nuclear overlapping area at mid-rapidity. The transverse energy density in each point inside the nuclear overlapping zone is supposed to be proportional to the impact-parameter dependent product of two nuclear thickness functions T_A in this point:

$$\varepsilon(r_1, r_2) \propto T_A(r_1)T_A(r_2), \quad (6)$$

where $r_{1,2}$ are the transverse distances between the centres of colliding nuclei and the parton production vertex. The rapidity dependent spreading of the initial energy density around mid-rapidity $y = 0$ is taken in the Gaussian-like form. The partonic energy loss depends also on the proper time τ_0 of matter formation and the number N_f of active flavors in the medium. Note that the variation of τ_0 value within its reasonable range has rather moderate influence on the strength of partonic energy loss. The jet quenching gets stronger at larger τ_0 due to slower medium cooling, which implies the jet partons spending more time in the hottest regions, and as a result the rescattering intensity some increases [27].

Another important ingredient of the model is the angular spectrum of medium-induced radiation. There is a number of recent theoretical achievements related to this subject (see, e.g., [34,57,58,59,60]). Nevertheless to the best of our knowledge there is no unique well-defined angular spectrum of emitted gluons in the current literature to be implemented in Monte-Carlo models unambiguously. This is one of main reasons leading to various approaches to modeling of medium-induced partonic energy loss in the existing event generators. Since the detailed Monte-Carlo treatment of the angular spectrum of medium-induced radiation is rather sophisticated and ambiguously determined, the simple parameterizations of the gluon distribution over the emission angle θ are used within PYQUEN,

to get some notion about possible effects related to angular structure and to illustrate our interpretation of the data. There are two basic limiting options in the model. The first one is the “small-angle” radiation,

$$\frac{dN^g}{d\theta} \propto \sin \theta \exp \left(-\frac{(\theta - \theta_0)^2}{2\theta_0^2} \right), \quad (7)$$

where $\theta_0 \sim 5^\circ$ is the typical angle of the coherent gluon radiation as estimated in [61]. This scenario results in very close predictions to those obtained under assumption that all gluons are emitted collinearly (along the direction of motion of radiating particle). The second option is the “wide-angle” radiation,

$$\frac{dN^g}{d\theta} \propto 1/\theta, \quad (8)$$

which is similar to the angular spectrum of parton showering in a vacuum without coherent effects [62]. The physical meaning of wide-angle radiation could be the presence of intensive secondary rescatterings of in-medium emitted gluons [24]. It may result in destroying the small-angle (BDMPS-like) coherence emission and significant broadening of gluon emission angular spectrum. This scenario allows us to estimate effects of radiation outside the typical jet cone. The collisional energy loss in PYQUEN is always “out-of-cone” loss. Such lost energy is considered as “absorbed” by the medium, because the major part of “thermal” particles knocked out of the hot matter by elastic rescatterings fly outside the typical jet cone [61].

The event-by-event Monte-Carlo simulation procedure in PYQUEN includes three main steps: the generation of initial parton spectra with PYTHIA and production vertexes at the given impact parameter; the rescattering-by-rescattering passage of each jet parton through a dense zone accompanied with gluon radiation and collisional energy loss; the final hadronization for jet partons and in-medium emitted gluons according to the standard Lund string scheme implemented in PYTHIA.

3 Results

PYQUEN model was applied to simulate medium-modified inclusive jet production at energy $\sqrt{s_{NN}} = 2.76$ TeV for different PbPb centralities. The radiative and collisional energy loss were taken into account. Two options for the angular spectrum of gluon radiation were considered, wide- and small-angle radiative loss. Hereafter let us call these options as “Scenario *W*” and “Scenario *S*” respectively. The discrimination between these two ultimate scenarios when analyzing various jet characteristics seems particularly interesting, because it allows one to get some notion about possible effects related to angular structure of medium-induced partonic energy loss. “Scenario *S*” results in very close predictions to those obtained under assumption that gluons are emitted collinearly, while “Scenario *W*” is useful to estimate effects of radiation outside the typical jet cone. At the same time a specific form of angular spectrum is not crucial for these two extreme cases,

only a part of the energy loss outside the typical jet cone is significant for the effects under consideration.

PYQUEN parameter values $T_0^{\max} = 1$ GeV, $\tau_0 = 0.1$ fm/c and $N_f = 0$ (gluon-dominated plasma) were used for our simulations. Such parameter settings allow the model to reproduce the LHC data on dijet transverse energy imbalance and nuclear modification factors of inclusive hadrons as wide-angle radiative and collisional energy loss are taken into account [27,28]. At that PYTHIA tune Pro-Q20 was utilized.

In the current paper we do not intend to do a complete “apples to apples” comparison of the model results with the data. Such kind of comparison for jet observables should contain full (or fast) simulation of detector responses, that has to work within the experiment’s software suite and it certainly cannot be done within the phenomenological paper. However we try to take into account the basic experimental effects (affecting the jet observables) in some simplified but reasonable ways. In order to include a jet reconstruction on the calorimetric level in our simulation, we apply the iterative cluster finding algorithm PYCELL implemented in PYTHIA [48]. Final state jets within cone size $R^{\text{jet}} = \sqrt{\Delta\varphi^2 + \Delta\eta^2} = 0.3$ with transverse energy $E_T^{\text{jet}} > 100$ GeV and pseudorapidity $0.3 < |\eta^{\text{jet}}| < 2$ were considered. The numerical results were compared with the CMS data on modification factors for jet shapes [43] and jet fragmentation function [44] using the same kinematic cuts as in the experiment. Note that the data have been obtained by more complicated way, using the anti- k_T algorithm [63], utilizing so-called particle-flow objects that combine tracking and calorimetric information. However we assume that the physical observables should be stable for different reasonable algorithms. For example, in [14] the calorimeter-based iterative cone algorithm was applied as a basic option for jet reconstruction, while the anti- k_T algorithm based on particle flow objects was used for a cross-check of the results. A good agreement between the results obtained with two algorithms has been found.

Another simplification in our simulation is not taking into account the high multiplicity background. The correct performance of jet reconstruction algorithms and background subtraction procedure is checked and verified in any such experimental analysis (including ones discussed in the current paper). So the measured physical observables are supposed to be stable with respect to the background fluctuations. Since attempt to reproduce the jet analysis procedure within the model by exactly the same way as in the experiment would require huge extra efforts without crucial influence on the results obtained, we believe that our simulation of experimental effects is enough to support our main physical conclusions.

At first we have checked that the overall suppression of inclusive jet rates for 10% of most central PbPb events as compared to the corresponding pp collisions (scaled to the number of binary nucleon-nucleon collisions) almost does not depend on E_T^{jet} , and is found on the level $R_{AA}^{\text{jet}} \sim 0.5 \div 0.55$ for “Scenario *S*” and $R_{AA}^{\text{jet}} \sim 0.4 \div 0.45$ for “Scenario *W*”. Both results are close to the ATLAS

measurements of the jet suppression factor [17,19] within statistical and systematic uncertainties of the data. Since no qualitative difference between “Scenario W” and “Scenario S” seen for the energy dependence of R_{AA}^{jet} (only numerical difference $\sim 20\%$ independently of E_T^{jet}), making unambiguous conclusions in favour of either scenario based on R_{AA}^{jet} measurements would be rather difficult. Our explanation for this is as follows. The naive expectation is that small-angle radiation will, in the first place, soften particle energy distributions inside the jet, increase the multiplicity of secondary particles, but (almost) will not affect the total jet energy. In such a case jet suppression could be significantly less pronounced than the one for wide-angle radiation. However the inevitable feature of any jet reconstruction algorithm is the separation of high and low transverse momentum particles (clusters) to treat them as extracted signal and subtracted background respectively. Thus softening of particle distribution inside the jet effectively results in loss of jet energy, and difference between two scenarios for jet suppression factors becomes not so pronounced.

Then we consider the jet internal structure. The radial jet profile may be characterized by the distribution of the transverse momentum inside the jet cone:

$$\rho(r) = \frac{1}{\delta r} \frac{1}{N_{\text{jet}}} \sum_{\text{jets}} \frac{p_T(r - \delta r/2, r + \delta r/2)}{E_T^{\text{jet}}}, \quad (9)$$

where $r = \sqrt{(\eta - \eta_{\text{jet}})^2 + (\varphi - \varphi_{\text{jet}})^2} \leq R^{\text{jet}}$ is the radial distance from jet particle to the jet axis, defined by the coordinates η_{jet} and φ_{jet} . Following CMS analysis procedure [43] the jet cone was divided into six bins with radial width $\delta r = 0.05$, and the transverse momentum of all charged particles with $p_T > 1$ GeV/c in each radial bin was summed to obtain the fraction of the total jet p_T carried by these particles. Then the results were averaged over the total number of found jets, N_{jet} .

The longitudinal jet profile usually is characterized by the jet fragmentation function $D(z)$ defined as the probability for a jet particle to carry a fraction z of the jet transverse energy. Often jet fragmentation function is measured in terms of variable $\xi = \ln(1/z) = \ln(E_T^{\text{jet}}/p_T)$, and it is normalized to the total number of jets, N_{jet} . The charged particles with $p_T > 1$ GeV/c in a jet cone were selected for the analysis [44].

Figure 1 shows the jet shape nuclear modification factors, $\rho(r)(\text{PbPb})/\rho(r)(\text{pp})$, for four centralities of PbPb collisions. The specific modification of radial jet profile in most central collisions due to a redistribution of the jet energy inside the cone is observed. It includes the excess at large radii, the suppression at intermediate radii, and unchanged (or slightly enhanced) jet core. PYQUEN (“Scenario W”) produces the similar modification close to the data (within the experimental uncertainties). At the same time PYQUEN (“Scenario S”) gives qualitatively very different result, such as excess at large and intermediate radii, and suppression for jet core. The similar situation appears for jet fragmentation function (figure 2). The same prominent features for the ratio of PbPb jet fragmen-

tation function to its pp reference seen in the data and in the PYQUEN (“Scenario W”): the excess at low p_T (large ξ), the suppression at intermediate p_T (ξ), and the indication on a some enhancement at high p_T (small ξ , the domain of leading particles). Note that recent ATLAS data on jet fragmentation function [45] supports the presence of excess at high p_T with more confidence (but this comparison was done with respect to peripheral PbPb events). As with jet shapes, PYQUEN (“Scenario S”) fails to reproduce measured jet fragmentation functions providing the suppression at high p_T .

In order to analyze the relative contribution of wide-angle radiative and collisional energy loss to the medium-modified intra-jet structure, two additional PYQUEN options were considered: wide-angle radiative loss only (without collisional loss) and collisional loss only (without radiative loss). The corresponding results for jet shape nuclear modification factors and jet fragmentation function are shown on figure 3 for 10% of most central PbPb collisions. As it could be expected, the contribution from wide-angle radiative energy loss dominates. So the option “wide-angle radiative loss only” provides much stronger modification of the jet profile than the modification obtained for the option “collisional loss only”. With all this the scenario with wide-angle radiative loss alone cannot match the data well, so taking into account both the contributions is necessary. Note that the relative weight between both contributions is not regulated specially in the model, but implicitly is determined by the physical assumptions when calculating radiative and collisional energy loss (equations 2 and 3) and by settled model parameter values (mostly an initial maximal temperature T_0^{max}).

4 Discussion

Let us discuss now the possible origin of a such specific medium-modified jet structure. In-medium emitted gluons are softer than initial jet partons, and fly at some angle with respect to the parent parton direction. Thus it is quite expectable that such “additional” gluons contribute to an excess of hadron multiplicity at low transverse momenta and jet radial broadening. On the other hand, the energy loss of initial jet partons reduces a number of hadrons at high and intermediate transverse momenta, such hadrons being strongly correlated with a jet axis. Then at first glance it should result in the suppression of hadron multiplicities in a jet core and at high p_T , which contradicts the data. However, in fact medium-modified jet structure at intermediate and high p_T is determined by the interplay of two effects. The first one is radial broadening and longitudinal softening due rescatterings and energy loss of jet partons. The second one is shifting down the jet energy due to “out-of-cone” energy loss. The energy loss of a jet as a whole results in the difference between the “initial” (non-modified) and final jet energies. Since more energetic jets initially are more collimated and particle p_T -spectrum in such jets is more harder, two above effects enter into competition. If the

contribution of wide-angle partonic energy loss to the total loss is large enough, the decrease in the yield of jet particles at high p_T and the broadening of a jet core can be compensated by significant jet energy “rescaling”, and converted into increase in the particle yield and (almost) unmodified radial profile at small radii. Such specific behavior of medium-modified jet fragmentation function at high p_T has been predicted some years ago in [64] (see also subsection 6.16.2 in [65]). The influence of measured jet fragmentation functions by the enhanced quark-to-gluon jet fraction can be also important [12].

Note that the parameterizations (7) and (8) for gluon angular spectrum may be rather facile to account all features of intra-jet activity in the data, moreover our treatment of calorimetric jet finding being inevitably simplified as compared with the realistic experimental procedure. However it does not affect the main physical message originating from the present studies: the data support the supposition that the intensive wide-angle (out the jet cone) partonic energy loss occurs in most central PbPb collisions, while the scenario with small-angle loss seems to be inconsistent with the data. This interpretation is also in the agreement with the results of our previous model analysis of medium-induced imbalance in dijet transverse energy [27]. As we already mentioned above, a specific form of angular spectrum is not so important here, only a part of the energy loss outside the typical jet cone affects this kind of jet observables. For example, in [64] we analyzed the relation between in-medium softening jet fragmentation function and suppression of the jet rates due to energy loss outside the jet cone without using the explicit form of angular spectrum at all. Within the current study, we have found that increasing the parameter θ_0 in (7) by factor ~ 3 results in similar modification of longitudinal and radial jet profiles as it is obtained in “Scenario W”. Thus since the large rise in typical radiation angle and its smearing in the parameterization (7) effectively reproduces the wide-angle radiation case (8), a particular form of angular spectrum cannot be verified unambiguously within our simulation.

Finally we would like refer to some other recent theoretical calculations for jet structure observables in PbPb collisions at the LHC. Jet fragmentation function was calculated and compared with the data in Refs. [34, 42, 66, 67]. JEWEL event generator [34] and hybrid strong/weak coupling jet quenching model [42] are successful in describing the basic trends seen in the data excepting low- p_T region. Hardening of the fragmentation function at high p_T in these models is a consequence of the depletion of softer jet particles. Effective 1+1 dimensional quasi-Abelian model [66] is able to reproduce low and intermediate p_T -region, and predicts unmodified fragmentation at high p_T . Jet fragmentation function [67] and jet shapes [58] were studied also with YaJEM event generator. It has been found that YaJEM results are qualitatively consistent with measurements of jet fragmentation function, while simulated jet broadening seems to be significantly stronger than in the data.

5 Conclusion

Modification of jet fragmentation function and jet shapes in PbPb collisions at $\sqrt{s_{NN}} = 2.76$ TeV with respect to the corresponding pp data has been analyzed in the frameworks of PYQUEN partonic energy loss model. PYQUEN simulations with wide-angle radiative and collisional energy loss provide a specific medium-induced modifications of longitudinal and radial jet profiles in most central collisions, which are close to experimentally observed ones. In spite of the contribution from wide-angle radiative loss to the medium-modified intra-jet structure is found to dominate, taking into account collisional loss is also necessary to match the data. Some excess in the yield of jet particles at high p_T and (almost) unmodified jet core may be explained by significant shifting down the jet energy due to “out-of-cone” energy loss. At the same time, the scenario with small-angle energy loss does not reproduce this effect, and so seems to be inconsistent with the data. We suppose that when the contribution of wide-angle energy loss into the total loss becomes large enough, the decrease in the yield of jet particles at high transverse momenta and the broadening of a jet core is compensated by significant jet energy “rescaling”, and converted into increase in the particle yield and (almost) unmodified radial profile at small radii. Such rescaling is not possible if small-angular loss is the dominant source of energy loss.

Together with other jet observables, the medium-modified jet structure seen in most central PbPb collisions at the LHC supports the presence of intensive wide-angle partonic energy loss, and can put strong constraints on the theoretical models of jet quenching. Future LHC data collected at increased energy and luminosity are expected to deliver more precise measurements of various jet characteristics in heavy ion collisions. This will allow us to study jet quenching mechanisms and properties of hot deconfined matter in more detail.

Acknowledgments

Discussions with M. Spusta and A.I. Demianov are gratefully acknowledged. We thank our colleagues from CMS collaboration for fruitful cooperation. This work was supported by Russian Scientific Fund (grant 14-12-00110).

References

1. D. d’Enterria, Landolt-Bornstein **23**, (2010) 471
2. U.A. Wiedemann, Landolt-Bornstein **23**, (2010) 521
3. A. Accardi, F. Arleo, W.K. Brooks, D. d’Enterria, V. Mucifora, Riv. Nuovo Cim. **32**, (2010) 439
4. A. Majumder, M. Van Leeuwen Prog. Part. Nucl. Phys. **66**, (2011) 41
5. I.M. Dremin, A.V. Leonidov, Phys. Usp **53**, (2011) 1123
6. Y. Mehtar-Tani, J.G. Milano, K. Tywoniuk, Int. J. Mod. Phys. A **28**, (2013) 1340013
7. A. Majumder, arXiv:1405.2019 [nucl-th]

8. I. Arsene, et al. (BRAHMS Collaboration), Nucl. Phys. A **757**, (2005) 1
9. B.B. Back, et al. (PHOBOS Collaboration), Nucl. Phys. A **757**, (2005) 28
10. J. Adams, et al. (STAR Collaboration), Nucl. Phys. A **757**, (2005) 102
11. K. Adcox, et al. (PHENIX Collaboration), Nucl. Phys. A **757**, (2005) 184
12. M. Spousta, Mod. Phys. Lett. A **28**, (2013) 1330017
13. G. Aad, et al. (ATLAS Collaboration), Phys. Rev. Lett. **105**, (2010) 252303
14. S. Chatrchyan, et al. (CMS Collaboration), Phys. Rev. C **84**, (2011) 024906
15. S. Chatrchyan, et al. (CMS Collaboration), Phys. Lett. B **712**, (2012) 176
16. S. Chatrchyan, et al. (CMS Collaboration), Phys. Lett. B **718**, (2013) 773
17. G. Aad, et al. (ATLAS Collaboration), Phys. Lett. B **719**, (2013) 220
18. B. Abelev, et al. (ALICE Collaboration), JHEP **1403**, (2014) 013
19. G. Aad, et al. (ATLAS Collaboration), Phys. Rev. Lett. **114**, (2015) 072302
20. G. Aad, et al. (ATLAS Collaboration), Phys. Rev. Lett. **111**, (2013) 152301
21. S. Chatrchyan, et al. (CMS Collaboration), Phys. Rev. Lett. **113**, (2014) 132301
22. S. Chatrchyan, et al. (CMS Collaboration), Eur. Phys. J. C **74**, (2014) 2951
23. J. Casalderrey-Solana, J.G. Milhano, U.A. Wiedemann, J. Phys. G **8**, (2011) 035006
24. G.-Y. Qin, B. Muller, Phys. Rev. Lett. **106**, (2011) 162302
25. C. Young, B. Schenke, S. Jeon, C. Gale, Phys. Rev. C **84**, (2011) 024907
26. D. Srivastava, J. Phys. G **38**, (2011) 055003
27. I.P. Lokhtin, A.V. Belyaev, A.M. Snigirev, Eur. Phys. J. C **71**, (2011) 1650
28. I.P. Lokhtin, A.V. Belyaev, L.V. Malinina, S.V. Petrushanko, E.P. Rogochaya, A.M. Snigirev, Eur. Phys. J. C **72**, (2012) 2045
29. B. Betz, M. Gyulassy, Phys. Rev. C **86**, (2012) 024903
30. T. Renk, Phys. Rev. C **85**, (2012) 064908
31. T. Renk, Phys. Rev. C **86**, (2012) 061901
32. T. Renk, Phys. Rev. C **88**, (2013) 014905
33. L. Apolinario, N. Armesto, L. Cunqueiro, JHEP **1302**, (2013) 022
34. K.C. Zapp, F. Krauss, U.A. Wiedemann, JHEP **1303**, (2013) 080
35. W. Dai, I. Vitev, B.-W. Zhang, Phys. Rev. Lett. **110**, (2013) 142001
36. J. Huang, Z.-B. Kang, I. Vitev, Phys. Lett. B **726**, (2013) 251
37. B.G. Zakharov, JETP Lett. **96**, (2013) 616
38. B.G. Zakharov, J. Phys. G **41**, (2014) 075008
39. K.M. Burke, et al., Phys. Rev. C **90**, (2014) 014909
40. J. Xu, A. Buzzatti, M. Gyulassy, JHEP **1408**, (2014) 063
41. Y. Mehtar-Tani, K. Tywoniuk, Phys. Lett. B **744**, (2015) 284
42. J. Casalderrey-Solana, D.C. Gulhan, J.G. Milhano, D. Pablos, K. Rajagopal, JHEP **1410**, (2014) 19
43. S. Chatrchyan, et al. (CMS Collaboration), Phys. Lett. B **730**, (2014) 243
44. S. Chatrchyan, et al. (CMS Collaboration), Phys. Rev. C **90**, (2014) 024908
45. G. Aad, et al. (ATLAS Collaboration), Phys. Lett. B **739**, (2014) 320
46. M. Cacciari, P. Quiroga-Arias, G.P. Salam, G. Soyez, Eur. Phys. J. C **73**, (2013) 2319
47. I.P. Lokhtin, A.M. Snigirev, Eur. Phys. J. C **45**, (2006) 211
48. T. Sjostrand, S. Mrenna, P. Skands, JHEP **0605**, (2006) 026
49. R. Baier, Yu. L. Dokshitzer, A.H. Mueller, S. Peigne, D. Schiff, Nucl. Phys. B **483**, (1997) 291
50. R. Baier, Yu. L. Dokshitzer, A.H. Mueller, D. Schiff, Phys. Rev. C **60**, (1999) 064902
51. R. Baier, Yu. L. Dokshitzer, A.H. Mueller, D. Schiff, Phys. Rev. C **64**, (2001) 057902
52. Yu.L. Dokshitzer, D. Kharzeev, Phys. Lett. B **519**, (2001) 199
53. J.D. Bjorken, Fermilab publication Pub-82/29-THY, 1982
54. E. Braaten, M. Thoma, Phys. Rev. D **44**, (1991) 1298
55. I.P. Lokhtin, A.M. Snigirev, Eur. Phys. J. C **16**, (2000) 527
56. J.D. Bjorken, Phys. Rev. D **27**, (1983) 140.
57. J. Casalderrey-Solana, Y. Mehtar-Tani, C.A. Salgado, K. Tywoniuk, Phys. Lett. B **725**, (2013) 357
58. R. Perez-Ramos, T. Renk, Phys. Rev. D **90**, (2014) 014018
59. A. Kurkela, U.A. Wiedemann, Phys. Lett. B **740**, (2015) 172
60. J.P. Blaizot, Y. Mehtar-Tani, M.A.C. Torres, arXiv:1407.0326 [hep-ph]
61. I.P. Lokhtin, A.M. Snigirev, Phys. Lett. B **440**, (1998) 163
62. Yu.L. Dokshitzer, V.A. Khoze, A.H. Mueller, S.I. Troian, *Basics of perturbative QCD* (Gif-sur-Yvette, France, Ed. Frontieres, 1991)
63. M. Cacciari, G.V. Salam, G. Soyez, JHEP **0804**, (2008) 063
64. I.P. Lokhtin, A.M. Snigirev, Phys. Lett. B **567**, (2003) 39
65. N. Armesto, et al., J. Phys. G **35**, (2008) 054001
66. D. Kharzeev, F. Loshaj, Phys. Rev. D **87**, (2013) 077501
67. R. Perez-Ramos, T. Renk, arXiv:1411.1983 [hep-ph]

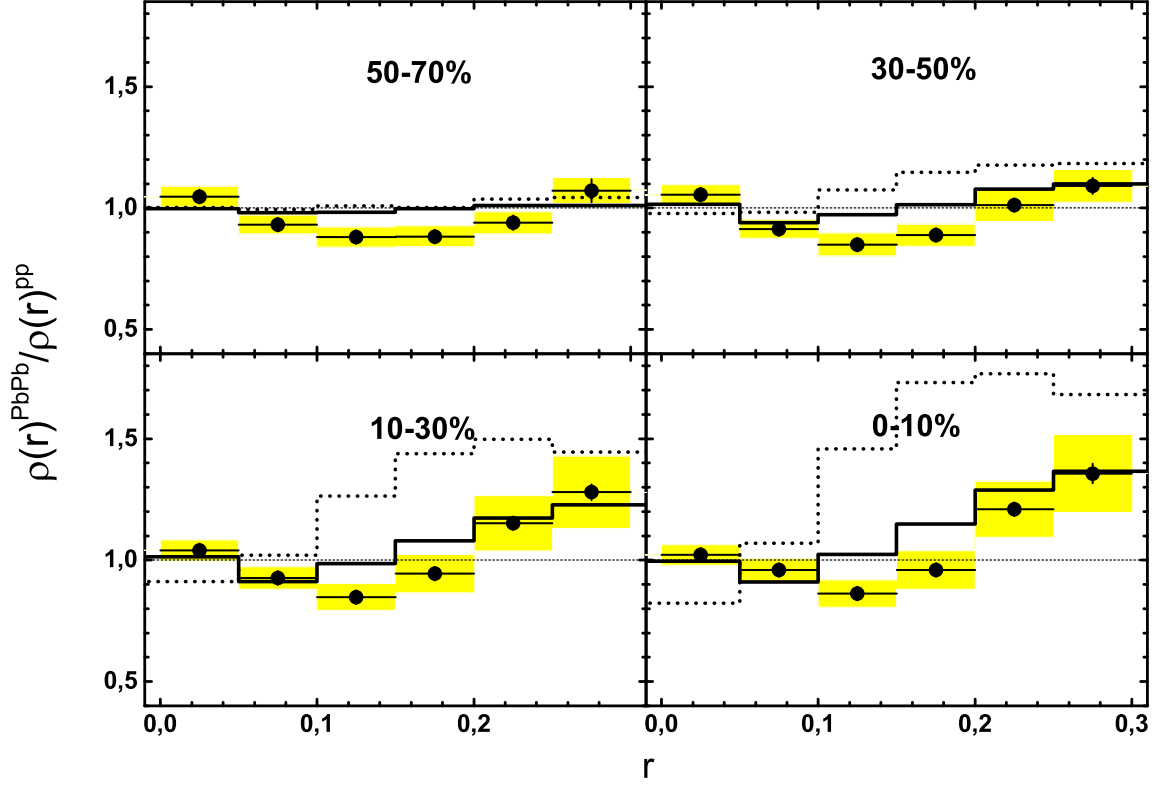


Fig. 1. Jet shape nuclear modification factors as a function of distance from the jet axis in PbPb collisions (four centralities) at $\sqrt{s_{\text{NN}}} = 2.76$ TeV for inclusive jets with $E_{\text{T}}^{\text{jet}} > 100$ GeV and pseudorapidity $0.3 < |\eta^{\text{jet}}| < 2$. The charged particles with $p_{\text{T}} > 1$ GeV/c in a jet cone $R = 0.3$ are included. The closed circles are CMS data [43], the error bars show the statistical uncertainties, and the boxes show the systematic errors. The solid and dashed histograms are simulated PYQUEN events for “Scenario W” (wide-angle radiative plus collisional energy loss) and “Scenario S” (small-angle radiative plus collisional energy loss) respectively.

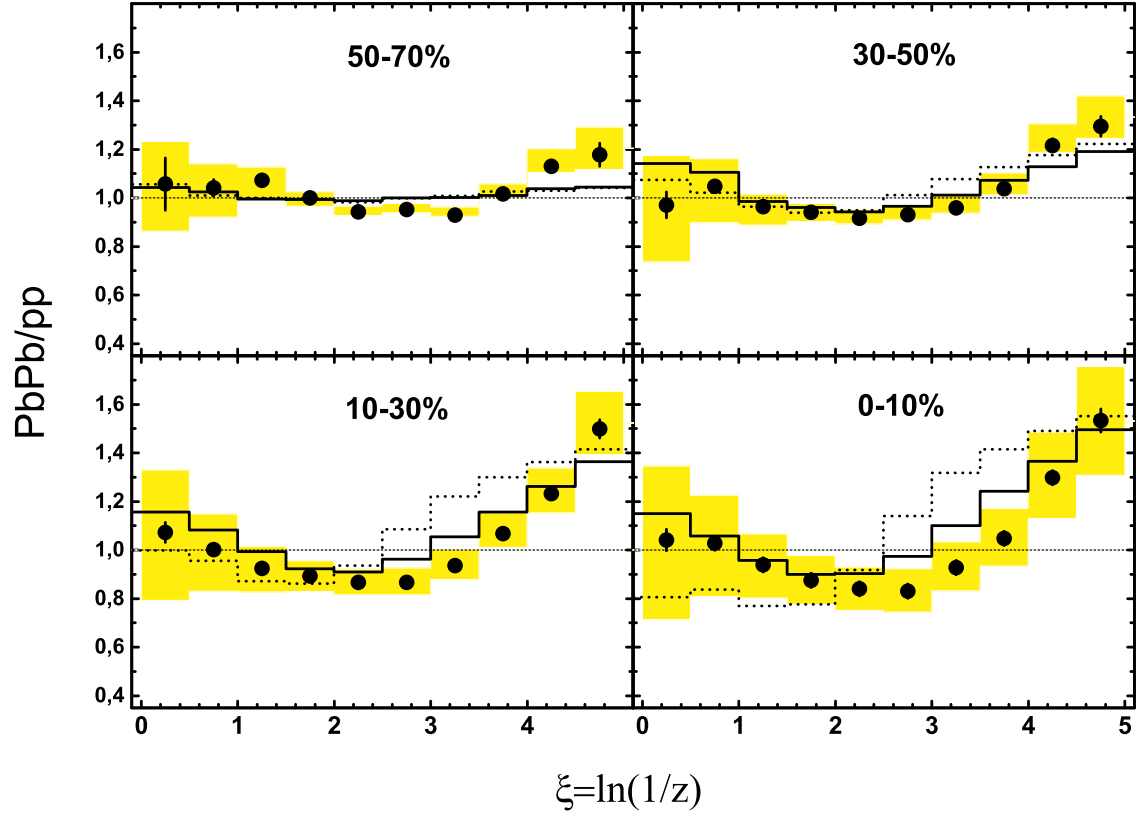


Fig. 2. The ratio of jet fragmentation function in PbPb collisions (four centralities) to its pp reference at $\sqrt{s_{NN}} = 2.76$ TeV for inclusive jets with $100 < E_T^{\text{jet}} < 300$ GeV and pseudorapidity $0.3 < |\eta^{\text{jet}}| < 2$. The charged particles with $p_T > 1$ GeV/c in a jet cone $R = 0.3$ are included. The closed circles are CMS data [44], the error bars show the statistical uncertainties, and the boxes show the systematic errors. The solid and dashed histograms are simulated PYQUEN events for “Scenario W” (wide-angle radiative plus collisional energy loss) and “Scenario S” (small-angle radiative plus collisional energy loss) respectively.

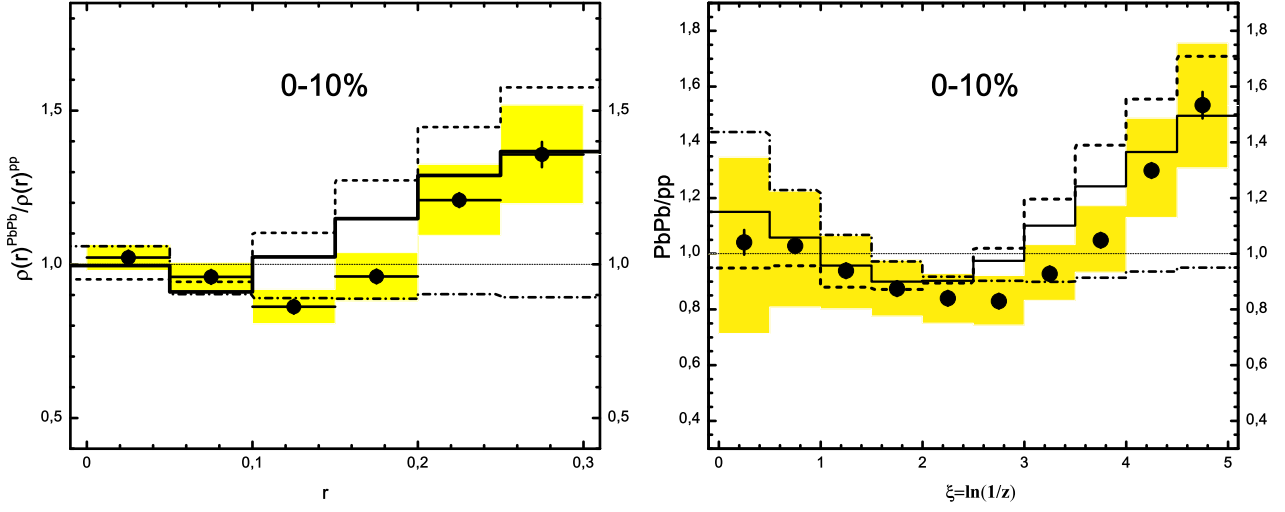


Fig. 3. Jet shape nuclear modification factor as a function of distance from the jet axis in PbPb collisions (left) and the ratio of jet fragmentation function in PbPb collisions to its pp reference (right) at $\sqrt{s_{\text{NN}}} = 2.76$ TeV (0-10% centrality) for inclusive jets with $E_{\text{T}}^{\text{jet}} > 100$ GeV and pseudorapidity $0.3 < |\eta^{\text{jet}}| < 2$. The charged particles with $p_{\text{T}} > 1$ GeV/c in a jet cone $R = 0.3$ are included. The closed circles are CMS data [43,44], the error bars show the statistical uncertainties, and the boxes show the systematic errors. The solid, dashed and dash-dotted histograms are simulated PYQUEN events for “Scenario W” (wide-angle radiative plus collisional energy loss), scenario “wide-angle radiative loss only” and scenario “collisional energy loss only” respectively.